


RESEARCH ARTICLE

Open Access



Parasitic resistance as a predictor of faulty anodes in electro galvanizing: a comparison of machine learning, physical and hybrid models

Mario Lovrić^{1,2*} , Richard Meister², Thomas Steck³, Leon Fadljević², Johann Gerdenitsch³, Stefan Schuster³, Lukas Schiefermüller³, Stefanie Lindstaedt^{1,2} and Roman Kern^{1,2}

*Correspondence:

lovric@tugraz.at

¹ Institute of Interactive Systems and Data Science, TU Graz, Inffeldgasse 16c, 8010 Graz, Austria
Full list of author information is available at the end of the article

Abstract

In industrial electro galvanizing lines aged anodes deteriorate zinc coating distribution over the strip width, leading to an increase in electricity and zinc cost. We introduce a data-driven approach in predictive maintenance of anodes to replace the cost- and labor-intensive manual inspection, which is still common for this task. The approach is based on parasitic resistance as an indicator of anode condition which might be aged or mis-installed. The parasitic resistance is indirectly observable via the voltage difference between the measured and baseline (theoretical) voltage for healthy anode. Here we calculate the baseline voltage by means of two approaches: (1) a physical model based on electrical and electrochemical laws, and (2) advanced machine learning techniques including boosting and bagging regression. The data was collected on one exemplary rectifier unit equipped with two anodes being studied for a total period of two years. The dataset consists of one target variable (rectifier voltage) and nine predictive variables used in the models, observing electrical current, electrolyte, and steel strip characteristics. For predictive modelling, we used Random Forest, Partial Least Squares and AdaBoost Regression. The model training was conducted on intervals where the anodes were in good condition and validated on other segments which served as a proof of concept that bad anode conditions can be identified using the parasitic resistance predicted by our models. Our results show a RMSE of 0.24 V for baseline rectifier voltage with a mean \pm standard deviation of 11.32 ± 2.53 V for the best model on the validation set. The best-performing model is a hybrid version of a Random Forest which incorporates meta-variables computed from the physical model. We found that a large predicted parasitic resistance coincides well with the results of the manual inspection. The results of this work will be implemented in online monitoring of anode conditions to reduce operational cost at a production site.

Keywords: Big data, Voltage, Random forest, Electroplating, Gravitel cell, Zinc coating, Steel

Introduction

Electro galvanizing is a well proven technology for producing corrosion-protected steel sheets with excellent surface quality, weldability and forming behavior [1]. Sometimes electro galvanizing is the only way to coat advanced high strength steels because it is a low temperature process and the mechanical properties of the steel substrate remain mostly unaffected. Electro galvanizing has some unique features like one-sided coating and low coating thicknesses (less than 3 μm) [2]. The anode's quality has a huge impact on the zinc thickness distribution and furthermore on the overall energy consumption. Therefore, the anodes underlie strict maintenance and have to be changed if degraded. Unfortunately, there is no method for online detection of anode quality, which can monitor critical anode properties to foresee the end of the anode's lifetime. But with the help of machine learning models the condition of anodes used in electro galvanizing lines can be monitored during their lifetime.

In steel manufacturing, the enormous progress of available machine learning techniques together with the remarkable increase of available processing power and memory at affordable price levels has spurred a significant number of applications, ranging from blast furnace molten iron quality prediction [3], blast furnace stock line detection [4], continuous casting sticker detection [5], coating weight control [6], and prediction of the mechanical properties of galvanized steel coils [7]. In particular, if the development of purely physics-driven models is too complicated or time-consuming, machine learning techniques are a viable alternative. However, despite the aforementioned achievements, steel manufacturing and heavy industry applications in general still pose significant challenges for the appliance of machine learning techniques. Typically, the amount of available labelled high-quality data is quite low. In such scenarios, it can be advantageous to use so-called physics-guided approaches as a kind of hybrid modelling technique.

Hybrid modelling has gained a lot of popularity recently as a proposed answer to the limitations of either purely data-driven or purely physics-driven model building. In hybrid modeling, the two approaches are systematically combined. There exists a variety of options how to combine these models, and we want to highlight some of the most prominent examples here. In a traditional Data Science setting, the domain knowledge (e.g., physical laws) is being exploited to shape the features which can be fed to data-driven models [8, 9]. There are also examples of using domain-specific knowledge for feature selection, such as the selection of top-relevant frequencies to detect misfires in engines [10]. Another example from the same domain demonstrates another strategy, where a physics-based simulation model is applied in order to generate a dataset, which in turn is used as training data for data-driven machine learning models [11]. Alternatively, a physics-driven and a data-driven model can also be developed independently, with their results being computed in parallel and later combined to form a single result [12]. The term sequential hybrid models is used to describe settings, where one of the model's outputs serves as input to the respective other type of model. This can mean that a physically inspired model, e.g. based on differential equations and real-world measurements, serves as input to a data-driven model, which then learns how to combine the physics-based results and the features [13].

Finally, an efficient data-driven model may be built to serve as an approximation to a complex physics-based model, in order to achieve a speed-up in the computations [14].

The latter setting is beneficial if the physics-based model provides sufficiently good results, but at the price of high computational complexity, which limits its applicability. The data-driven approximation provides a rough estimate of the results, but with the advantage of a much lower computational complexity and may guide the exploration process. One domain, where this is of particular importance, is material science, where due to the size of the search space, data-driven machine learning models are used to identify the most promising regions of the input space, which are then further analyzed using the more exact knowledge-driven model, leading to considerable speed-ups [15, 16]. Physics-based knowledge has also been exploited to inform the design of machine learning algorithms and architectures, going back to the inception of Convolutional Neural Networks, which exploit spatial neighborhood to achieve a sparse parameter space. Recently, more complex physics-derived constraints have been integrated directly into the network architecture, for example in the form of physics-informed convolutions [17]. This approach of constraining a machine learning algorithm is not limited to deep learning architectures, but can also be successfully applied to simpler models, like linear systems [18].

Finally, also the output stage of a machine learning algorithm can be adapted for hybrid-modelling [19]. For example, by adapting the loss function to replace the classical supervised scenario of labelled training examples with constraints derived from physical laws [20]. Karpatne et al. [21] proposed a rigorous scientific framework combining those different approaches, which they coined theory-guided data science. Their motivation is two-fold: first they attempt to increase the interpretability of data-driven, black-box models and, second, they intend to constrain data-driven models. The latter is aimed at improving the generalization ability of data-driven methods and to prevent physically inconsistent models. They outline procedures, how different parts of the model building process can be enhanced via theory-guided design, ranging from choosing appropriate link functions to selecting appropriate regularization functions. Subsequently, these methods have been applied specifically on deep neural networks [22]. Complementary approaches utilize physics-based theories to aid the interpretability of black-box models. As an example, Lei et al. [23] studied Convolutional Neural Networks by utilizing quantum mechanics, energy models and thermodynamic entropy to gain a deeper understanding of the intrinsic functionality of deep neural networks.

Our aim and contributions

To the best of our knowledge, this paper is the first to present a simplified physical model of the rectifier voltage in a large-scale electro galvanizing unit. This report is also the first to implement the use of the physical model for labelling of training and testing areas in an electro galvanization production line and employ sophisticated machine learning methods to predict the baseline rectifier voltage. We claim that aged or mis-installed anodes can be identified based on the presence of parasitic resistances, which are indirectly represented by a difference between theoretical (baseline) and measured voltage (parasitic voltage). In order to do that, the theoretical voltage was calculated based on a simplified physical model and alternatively predicted by machine learning from the electrical current, steel strip and electrolyte parameters. A comparison between the results

of the physical and machine learning model and the use of meta-variables from the physical model in hybrid machine learning models is rounding off our discovery.

Materials and methods

Process unit

The electro galvanizing line was previously described in [2, 24]. More details on the products and technology involved can be read in [1] while the GRAVITEL[®] plating cells are covered in [25, 26]. A schematic drawing of the electro galvanizing line is depicted in Fig. 1. It consists of 12 vertical cells with four anodes each. In the entry section the steel strips are welded together to form an endless strip. The looper installed downstream compensates short downtimes during welding in the entry section. The strip is straightened by the tension leveler. A multistage process to produce a clean and grease-free surface is implemented for pre-treatment.

This is an important precondition for the application of homogeneous zinc layers with good adhesion. In the plating section the strip passes 12 GRAVITEL cells in which zinc from the electrolyte is deposited on the surface due to the application of high electrical currents. This patented cell design allows single-sided or double-sided galvanizing of the strip. The conductor rolls and the sink roll direct the strip between the anode plates mounted on the anode boxes. One rectifier supplies two anodes, which are located on the top and the bottom side of the strip, as depicted in Fig. 2. The electrolyte is pumped into the wedge-shaped space between anode and strip and flows downward as pulled by gravity—similar to a cascade. Under the influence of the applied DC voltage, zinc ions move from the electrolyte to the strip, where they are deposited. In the post-treatment section, the strip surface is treated with various chemicals to obtain improved corrosion resistance and good paintability. Subsequently, the strip is rinsed and dried with hot air, and the thickness of the zinc coating is measured. In the inspection stand, surface inspection and strip marking are carried out. Upon request, the strip is additionally oiled (corrosion protection, forming behavior). Finally, the strip is coiled, cut from the endless

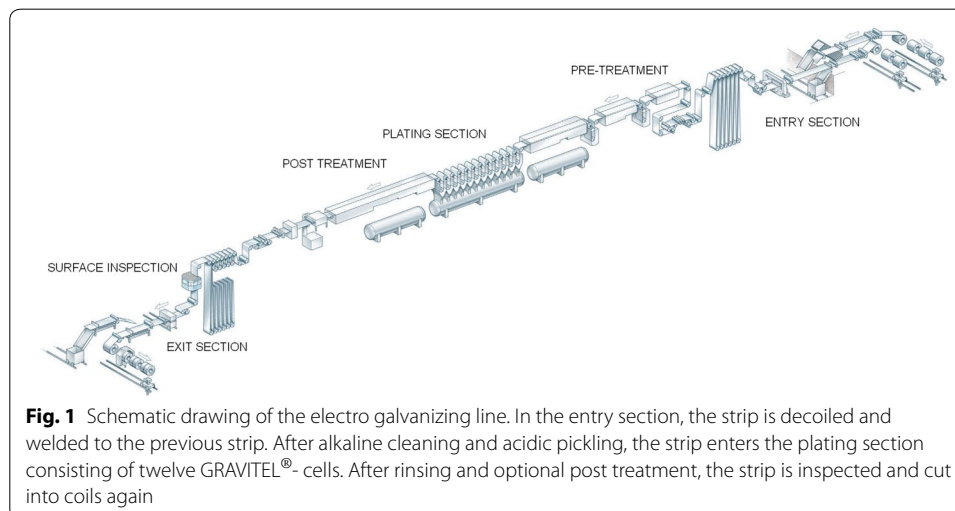


Fig. 1 Schematic drawing of the electro galvanizing line. In the entry section, the strip is decoiled and welded to the previous strip. After alkaline cleaning and acidic pickling, the strip enters the plating section consisting of twelve GRAVITEL[®]- cells. After rinsing and optional post treatment, the strip is inspected and cut into coils again

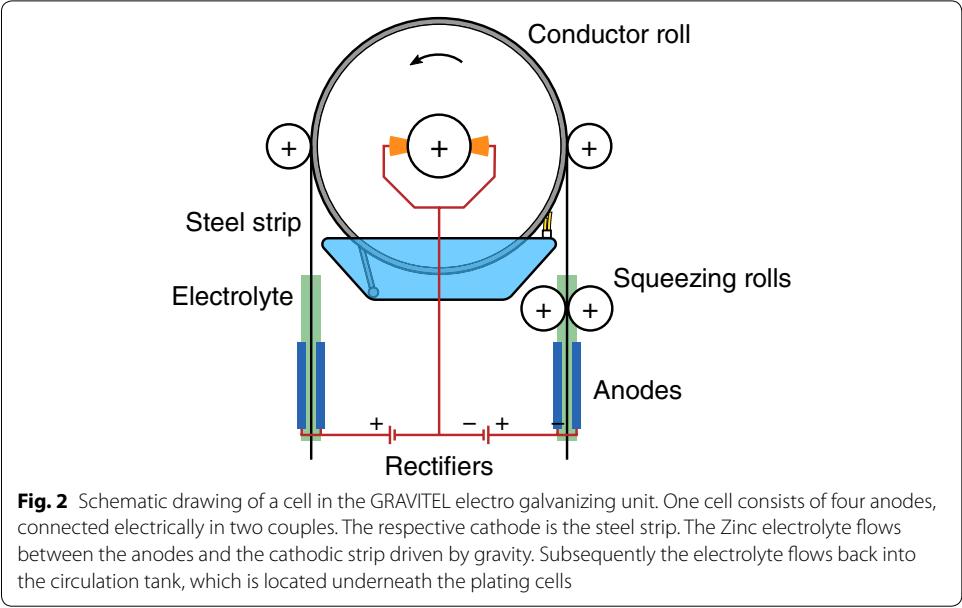


Fig. 2 Schematic drawing of a cell in the GRAVITEL electro galvanizing unit. One cell consists of four anodes, connected electrically in two couples. The respective cathode is the steel strip. The Zinc electrolyte flows between the anodes and the cathodic strip driven by gravity. Subsequently the electrolyte flows back into the circulation tank, which is located underneath the plating cells

Table 1 General process parameters in the galvanizing unit, described previously in [24, 26]

| Process parameter | Characteristics |
|----------------------------|---|
| Rectifier voltage | 11.228 ± 2.525 V (mean ± std.dev.) |
| Line speed | < 120 m/min |
| Anode type | Insoluble Ti anodes with IrO ₂ coating |
| Anode strip gap | 8 mm |
| Anode dimensions | 995 mm × 1650 mm |
| Electrical current density | < 150 A/dm ² |
| Electrolyte flow per cell | < 1000 m ³ /h |

strip and weighed. In the exit section, too, a looper helps to compensate short down-times (cutting). Some production parameters are presented in Table 1.

Anode aging

Anode aging has a variety of causes, amongst which the most important are strip contact, abrasion, corrosion by electrolyte, and human caused error like mis-installation. The anodes have a typical lifetime of 3–12 months in the cell, until they are removed based on the results of the visual inspection. The inspection procedure is conducted on a monthly basis. During inspection the strip is stopped and electro galvanizing is conducted in a static manner so that the current anode activity is reflected on the strip. The strip segments are subsequently photographed and evaluated visually by a team of process experts and technicians. Typical pictures of strip segments corresponding to “good” and “bad” anode conditions are shown in Fig. 3. This inspection procedure is costly, time

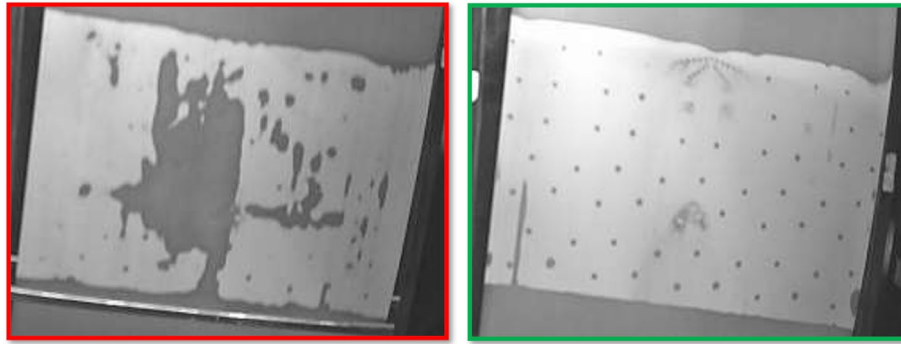


Fig. 3 Photographs of the plated strip taken from a “bad” (left) and a “good” anode condition (right). The right picture shows signs of wear. The photographs are evaluated manually by a team of experts

Table 2 Data included in the analysis

| Variable name | Sensor/measurement description | Use |
|---------------------------------|--|------------|
| Fe concentration in electrolyte | ICP-OES | Predictive |
| pH of the electrolyte | Potentiometric (pH sensor) | Predictive |
| Na concentration in electrolyte | ICP-OES | Predictive |
| Zn concentration in electrolyte | ICP-OES | Predictive |
| Electrolyte temperature | Pt-100 | Predictive |
| Width of steel strip | Tactile width measurement | Predictive |
| Thickness of steel strip | Radiometric | Predictive |
| Specific resistance | Current–Voltage determination (4-point method) | Predictive |
| Rectifier current | Potential drop at shunt | Predictive |
| Rectifier voltage | Potential | Target |

The variables are divided into three groups: electrolyte parameters, strip parameters, current characteristics. Out of these, nine parameters will be used as predictive variables

consuming, and depends on the skills of the plant staff. This was the motivator to implement predictive modelling of the rectifier voltage to assess the anode condition and find the correct time for replacing them.

Data acquisition and preparation

The data used in this study was collected on one exemplary rectifier unit equipped with two anodes over the course of 22 months with a frequency of one sample every 10 s. The dataset consists of one target variable (voltage) and nine predictive variables which are given in Table 2. The data processing and regression model training was performed using our pre-developed scripts written in Python [27].

The data was filtered prior to analysis, i.e. data segments were chosen where no external disturbances or maintenance occurred (determined by in-house records), where the production is set to double-sided galvanization (which accounts for up to 95% of production time) and where the sheet rolling speed was held above 35 m/min. Additional filtering is based on valid ranges for individual parameters, i.e. pH 0–14 and electrolyte temperature 40.0–100.0 °C. The electrolyte values were determined in the laboratory in eight-hour intervals by replicated measurements. The respective analytical methods are mentioned in Table 2. The laboratory features were linearly imputed to the 10 s intervals.

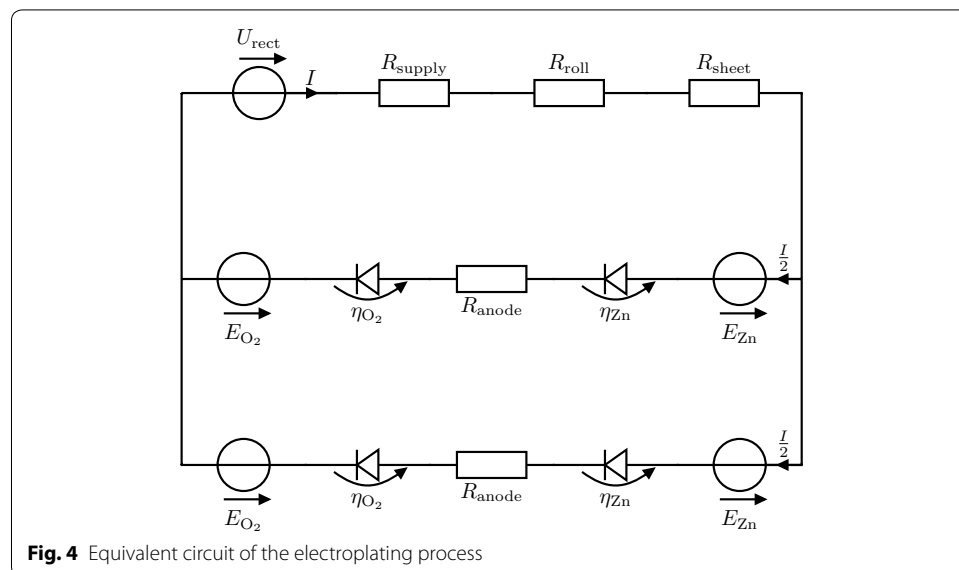
A simplified physical model

For the calculation of the baseline voltage, i.e. the voltage during good anode conditions, we developed a physical model based on electrochemical and physical laws. The electrical circuit of a single cell for electro galvanizing in a steady state can be approximated by the system shown in Fig. 4.

- U_{rect} is the driving voltage generated by the rectifiers and applied across the whole cell.
- R_{supply} is the resistance of the cables connecting the anodes and the conductor roll to the rectifier.
- R_{roll} is the resistance of the conductor roll itself and the transition resistance from the conductor roll to the steel sheet (see the schematic in Fig. 2).
- R_{sheet} models the resistance within the steel sheet from the conductor roll down to the electrolyte and depends on steel quality and strip thickness.

The circuit then splits into two parallel branches, as in the cases we investigated both sides of the strip were plated.

- The *electrochemical potential of zinc deposition* (E_{Zn}) remains nearly constant during operation and causes a voltage drop of about 0.76 V [28].
- The high current densities typically applied in electro galvanizing lines are far away from the equilibrium potential and therefore an additional potential η_{Zn} has to be added. This overpotential can be calculated using the Tafel equation [29].



- R_{anode} is the resistance of the electrolyte. It mainly depends on the distance between anode and steel strip and on the specific resistance of the electrolyte. The inverse of the specific resistance $\sigma_{\text{electrolyte}}$, can be calculated by the following empirical equation [30]:

$$\sigma_{\text{electrolyte}} \approx 90.9 - 0.089 c_{\text{Zn}} + 0.705 c_{\text{Na}} - 36.1 pH + 1.22 T - 0.00948 c_{\text{Zn}} c_{\text{Na}} + 0.107 pH c_{\text{Zn}} + 0.203 pH c_{\text{Na}} + 0.0145 c_{\text{Na}} T \quad (1)$$

- The electrochemical potential of oxygen evolution (E_{O_2}) causes a voltage drop of 1.23 V [29].
- Analogous to η_{Zn} , η_{O_2} is the overpotential between the electrode and the electrolyte caused by the kinetics of the oxidation reaction of H_2O to O_2 and H^+ . Both overpotentials are typically < 0.2 V.

From Fig. 4, an equation for theoretical rectifier voltage can be derived by simply adding up all voltage drops in the circuit (Eq. 2).

$$\begin{aligned} U_{\text{rect}} &= I \left(R_{\text{supply}} + R_{\text{roll}} + R_{\text{sheet}} + \frac{R_{\text{anode}}}{2} \right) + E_{\text{O}_2} + E_{\text{Zn}} + \eta_{\text{O}_2} + \eta_{\text{Zn}} \\ &= I \left(\frac{\rho_{\text{Cu}} L_{\text{supply}}}{A_{\text{supply}}} + \frac{\rho_{\text{roll}}}{b} + \frac{h + h_{\text{anode}}}{bd} \rho_{\text{sheet}} + \frac{w_{\text{top}} + w_{\text{bottom}} - d}{4bh_{\text{anode}}} \sigma_{\text{electrolyte}} \right) \\ &\quad + E_{\text{O}_2} + E_{\text{Zn}} + \frac{RT}{F} \sum_{k \in \{\text{Zn}, \text{O}_2\}} \left(\frac{1}{\alpha_k z_k} \log \frac{I}{2bh_{\text{anode}} j_{0,k}} \right) \end{aligned} \quad (2)$$

If I and U_{rect} —along with all the other relevant parameters—are measured, the difference between the calculated and measured rectifier voltage can be used to detect parasitic resistances—like aged anodes—within the circuit. A detailed explanation of the physical model is presented in Additional file 1.

Machine learning

For prediction of baseline rectifier voltage, we employed three different regression algorithms, namely Random Forest (RF) regression, AdaBoost (ADA) regression and partial least-squares (PLS) regression. Our choice of regression algorithms includes both linear and non-linear regressors, with the first two (RF, ADA) being considered non-linear black box ensemble methods, which gained popularity in industrial settings due to their prediction quality, little preprocessing effort and model tuning, as well as fast parallel training [30, 32]. Ensembles use the advantage of training many weak learners and average the predictions; the weak learners employed are commonly, but not exclusively, variations of decision trees aggregated either through boosting (sequential training) or bagging (parallel with random sub-sampling). Recently, ensemble methods performed best in machine learning and data science global challenges [33, 34].

Partial least squares

In PLS we want to find the multidimensional direction in the X-space (predictive variables) that explains the maximum multidimensional variance direction in the Y (target variable) [35]. The PLS method compresses the X-space to a set of vectors called latent components from the original X-space and builds a linear multivariable regression model for the target. A detailed overview of the method is presented in Refs. [35, 36].

Ensemble regressors

The Random Forest algorithm, conceptualized by Breiman [37], achieves prediction by exploiting bagging. The basis (weak learner) for RF is the decision tree algorithm. The independence between the individual weak learners reduces bias in the models, while variance can be controlled for by carefully optimizing weak learner hyperparameters, such as tree depth. Besides their good performance, RF accepts many feature representations and thus yields reduced preprocessing efforts, which makes them convenient for use in many applications, including manufacturing. Due to the fact that trees can be trained in parallel, a major advantage of RF is parallelization when used in high-throughput computing infrastructures.

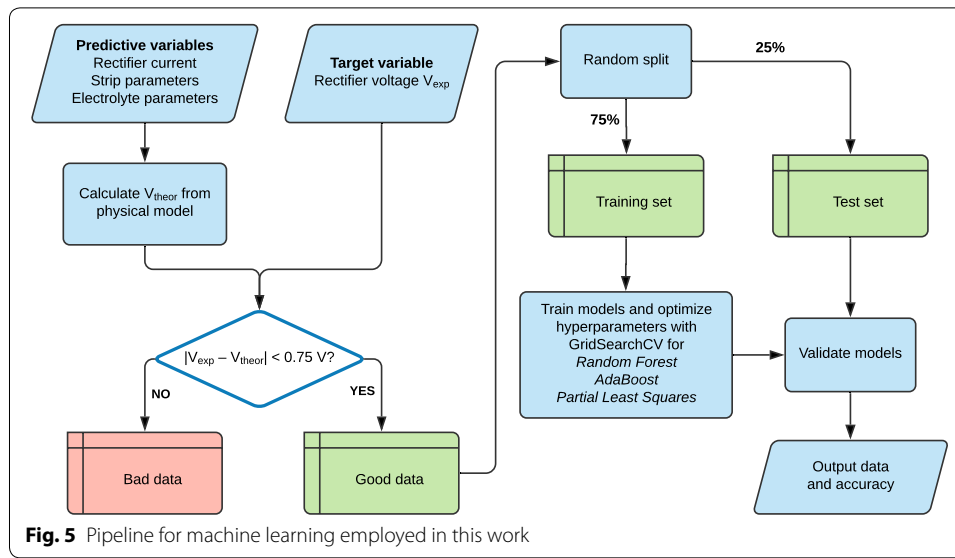
AdaBoost (adaptive boosting) [38] is based on sequential training on sub-samples where each instance (weak learner) is built in order to raise the importance of samples which have been mis-predicted in previous instances in the sequence. The final ensemble is then averaged with a weight based on accuracy of the instances in the sequence. A comparison of the two algorithms with a more detailed description is presented in Ref. [32].

Hybrid models

The hybrid models, as described in the introduction, comprise a combination of predictors based on physical and machine learning models. In this work, we employed the described physical voltage models to generate meta-variables which were used in the machine learning models (PLS, RF, ADA) to improve the prediction quality. To this end, all of the variables calculated in Eqs. 1–2 which were not in the baseline data set were used as additional inputs to the three regressors.

Model training and validation

We used scikit-learn [39] as implementation of the algorithms in our work. The baseline rectifier voltage was set as the target variable, with the other variables in Table 2 being predictive variables and meta-variables for the hybrid models. The data was divided into “good” and “bad” segments. The segments were labelled according to the difference of theoretical to measured voltage and according to results from the manual inspection of the anodes’ condition (see “Results of the physical model and data labeling” section). From the “good” segments (a data set of ~1.06 million measurements) a training set (75%) and a validation set (25%) were chosen at random. The validation set was held out until model validation when the model was evaluated. The complete model pipeline is presented in Fig. 5. All models were trained on an in-house big data server described in [40]. The evaluation of the models was conducted using the root mean squared error (RMSE, Eq. 5), the R -squared score (R^2 , Eq. 6), and mean absolute error (MAE, Eq. 7).



$$SS_{\text{tot}} = \sum_{i=1}^n (y_i - \bar{y})^2 \quad (3)$$

$$SS_{\text{res}} = \sum_{i=1}^n (\hat{y}_i - y_i)^2 \quad (4)$$

$$\text{RMSE} = \sqrt{\frac{SS_{\text{res}}}{n}} \quad (5)$$

$$R^2 = 1 - \frac{SS_{\text{res}}}{SS_{\text{tot}}} \quad (6)$$

$$\text{MAE} = \frac{\sum_{i=1}^n |y_i - \hat{y}_i|}{n} \quad (7)$$

For optimizing hyperparameters we used grid search [41] with tenfold cross validation on the training set, which showed good results in our previous work [27]. The hyperparameters for the grid search are presented in Additional file 1: Table S1.

Results and discussion

Results of the physical model and data labeling

We calculated the theoretical voltage based on the simplified physical model (Eqs. 1–2) in the section "A simplified physical model" given the electrical current, steel strip and electrolyte parameters. The assumption is that, from the difference of measured to theoretical voltage, one can reveal the appearance of parasitic resistance, which indicates bad anode conditions or mis-installation. Figure 6 shows a time series plot of the voltage difference (measured–theoretical), which can be seen as “parasitic voltage”

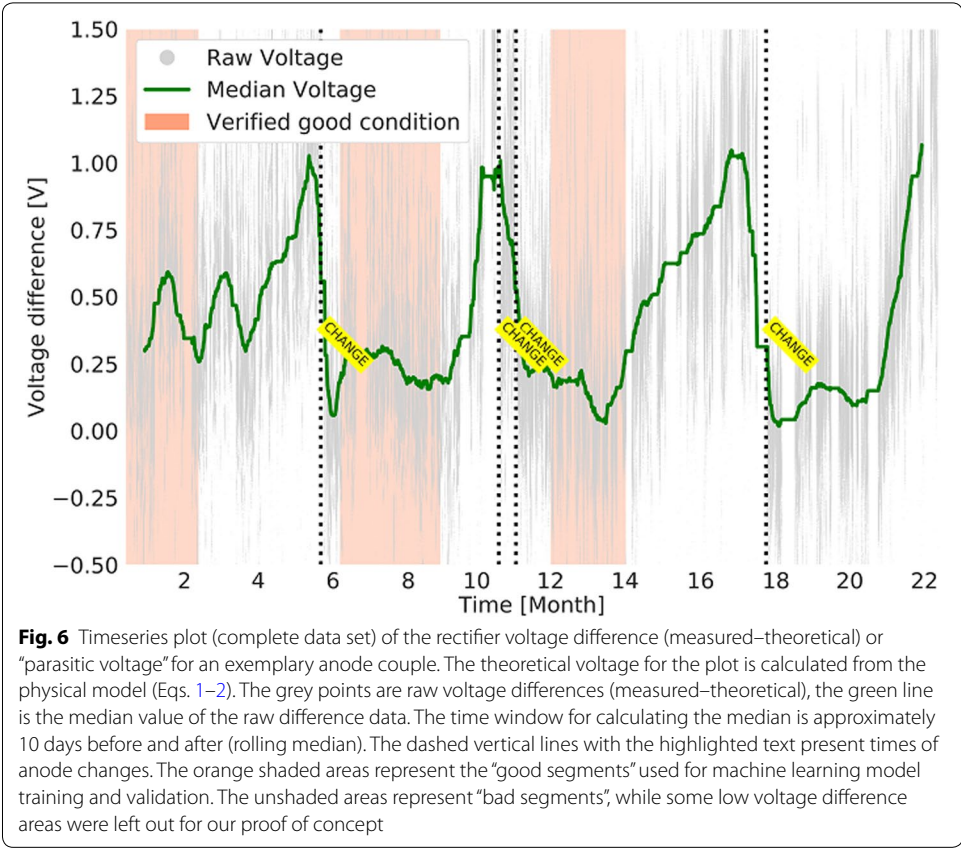
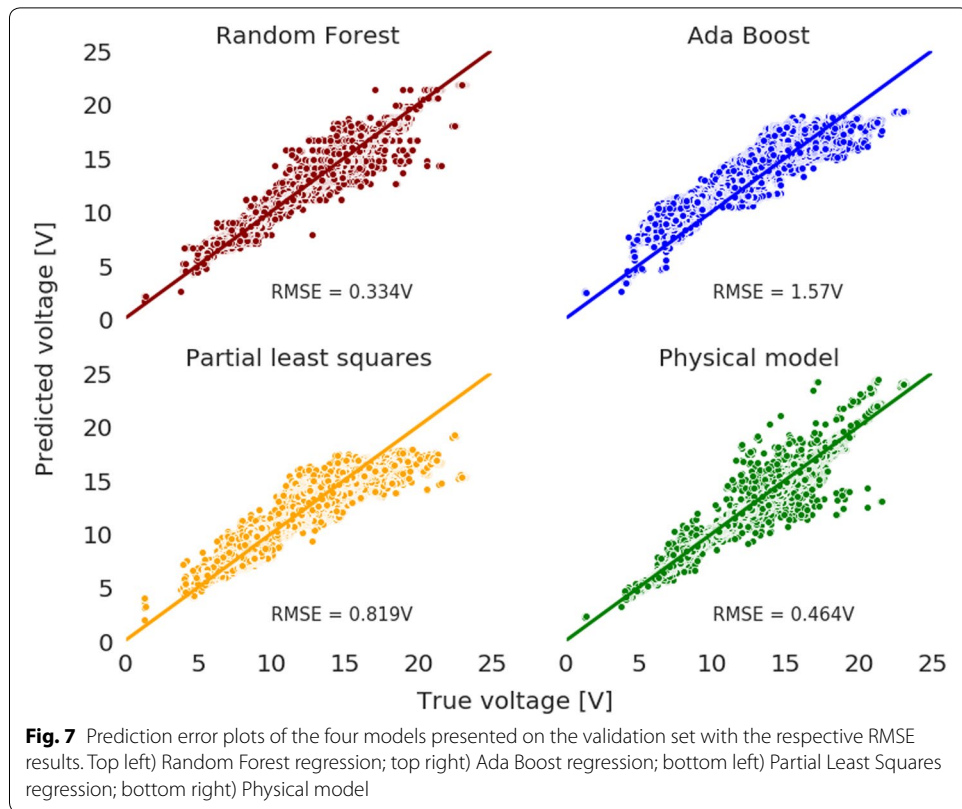


Fig. 6 Timeseries plot (complete data set) of the rectifier voltage difference (measured–theoretical) or “parasitic voltage” for an exemplary anode couple. The theoretical voltage for the plot is calculated from the physical model (Eqs. 1–2). The grey points are raw voltage differences (measured–theoretical), the green line is the median value of the raw difference data. The time window for calculating the median is approximately 10 days before and after (rolling median). The dashed vertical lines with the highlighted text present times of anode changes. The orange shaded areas represent the “good segments” used for machine learning model training and validation. The unshaded areas represent “bad segments”, while some low voltage difference areas were left out for our proof of concept

Table 3 Hyperparameters chosen by grid search for the base regressors (Additional file 1: Table S1)

| | |
|---------------------------------|--|
| Partial Least Square Regression | Max iterations = 200, N components = 2 |
| Random Forest Regression | Max depth = 8, No. estimators = 200, Min samples split = 200, Max samples = 0.5 |
| Ada Boost Regression | DecisionTreeRegressor (Max depth = 2), No. estimators = 1000, Loss = Square, Learning rate = 1 |

or voltage which cannot be explained by other contributions. The moments at which the anodes were changed are shown by vertical dashed lines. It can be observed that anodes got replaced by maintenance personnel about the same time the median voltage difference (parasitic voltage) was at ~1 V. The training periods (shaded in orange color) for machine learning were determined at times when the voltage difference was low, i.e. below 0.6 V, and where the maintenance personnel estimated anode condition as good. From the shaded areas containing data with good anode condition (which represent model training and validation sets together), 25% of data was chosen by random sampling for validation. The non-shaded areas were used for the proof of concept. The RMSE of the theoretical voltage calculated by the physical model on the validation set is 0.464 V. The area from month 18 onwards demonstrates the concept very well since the model assigned low differences to a fresh anode exchanged in month 18.



Results of the machine learning models

We trained three different machine learning models described in the "Machine learning" section. The optimal hyperparameters chosen by grid search are presented in Table 3.

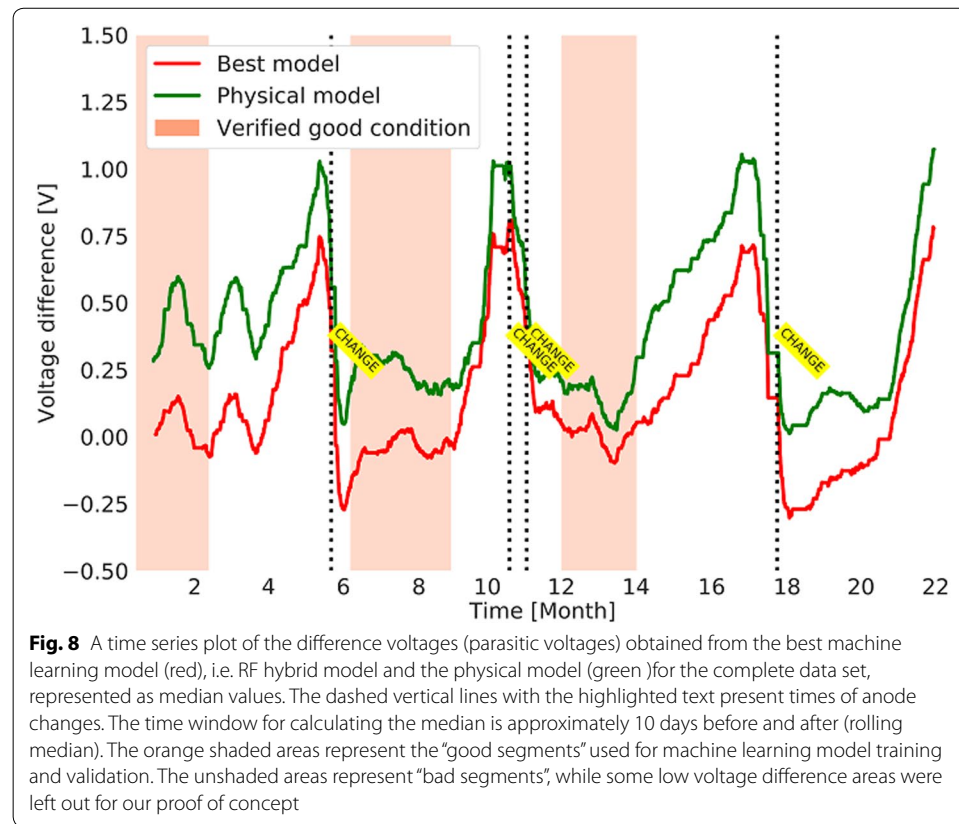
The predictive quality was evaluated on the validation sets. Figure 7 shows model residual plots. For comparison, the respective root mean square error values are included in the subplots. RF shows the best prediction on the validation set with a RMSE of 0.334 V. It is followed by the physical model with an RMSE of 0.464 V, PLS RMSE 0.819 V and ADA as the worst performing model with an RMSE of 1.570 V. From the plots in Fig. 7 it is clear that RF and the physical model have a higher error in the upper voltage region with no obvious global patterns in error distribution. They also appear to be less prone to potential outliers. ADA and PLS appear to have failed in fitting the data as the point cloud seems to experience a curved structure.

It was however expected that PLS will show less scattered points (outliers) since it can extrapolate better than Random Forest which is binning data amongst the known instances. Furthermore, RF has the hyperparameter "min samples" chosen to be 200, meaning there are 200 instances binned to one voltage value. ADA shows poor behavior with this data set.

The hybrid models were trained with 7 additional meta-variables capturing theory-driven information. Even though the additional variables are derived from the original ones (Table 1), we observed an improvement in the models' performance (Table 4). All models were improved through addition of meta-variables from the theoretical model, which adds electrochemical and physical knowledge to the models. This may have

Table 4 Results of all models on the validation sets by means of the scores calculated from Eqs. 5–6

| | R2 Score Baseline | MAE | RMSE | R2 Score Hybrid | MAE | RMSE | Δ RMSE Hybrid- Baseline |
|----------------|----------------------|-------|-------|--------------------|-------|-------|--------------------------------------|
| PLS | 0.895 | 0.610 | 0.819 | 0.964 | 0.308 | 0.481 | − 0.34 |
| Ada Boost | 0.614 | 1.302 | 1.570 | 0.583 | 1.479 | 1.632 | 0.06 |
| Random Forest | 0.983 | 0.232 | 0.334 | 0.989 | 0.185 | 0.263 | − 0.07 |
| Physical model | 0.966 | 0.337 | 0.464 | | | | |



allowed weak learners (RF and ADA) to produce better suiting splitting criteria and thus allowed for a better fit. Even though we employed three different metrics for result evaluation, the metrics are following the same pattern with RF showing the best performance in all of them. This can be assigned to the size of the data set, i.e. with a count of $\sim 265,000$ measurements in the validation set the metrics will be less sensitive to outliers than is the case with using a variety of metrics small data sets. The improved performance of RF over boosting algorithms (ADA herein) was also observed in prior work [30, 42]. Figure 8 shows a visual comparison of the median voltage differences predicted by the physical model (measured–theoretical) and the one predicted by means of the best model (Hybrid RF). The model was used to predict also the “bad sectors” which are unshaded areas in the plot.

It can be seen that overall, the best model calculated a lower baseline voltage, which is expected to be more realistic especially after the installation of fresh anodes. The unexpected lower voltage from month 18 onwards is assigned to a novel type of anode coating tested in the unit (which was not available in the training set). Both models show slightly lower median voltage.

Concept transfer and limitations

Our proposed concept can be transferred to any setting where existing physical models are employed but still have limitations in predictive quality. It is commonly seen that manufacturing plants employ physical models to describe dynamic processes in their individual production units. With inclusion of metavariables derived from or generated within physical models, one can improve data-driven predictions. This can be considered a feature engineering method. The methodology can be applied to any condition monitoring setup where the measured value, descriptive of a condition (a target variable), differs from predicted or physically modelled baseline caused by suboptimal working conditions. One has to be able to clearly determine the target variable (a quantified condition) and its possible predictors. Early classification in condition monitoring can reduce material and energy cost. With the use of ensemble regression models like Random Forest and AdaBoost, one can improve predictive power and reduce preprocessing time, since the models work well with heterogeneous data. The simplified data processing can therefore reduce the efforts in creating online and semi-online automated learning pipelines.

Some of the limitations of this approach will be explored in future research, such as the development of a universal model for all rectifiers; the removal of local outliers per strip prior to training; automated data labelling; the inclusion of additional process variables which are not present in the physical model. The same limitations can be transferred to other use cases where one has more data available in the system than those which are being considered as co-variables of the target variable. Furthermore, often industrial settings have more than one operating/processing unit of the same kind, which means universal models for all units might be desirable. An important aspect when modelling such systems are product and expendable material properties which, if changed, can cause drift in the covariance matrix. Besides that, process units can age as well and in case of such a dynamic system be influenced by corrosion and other tribological effects. In the model presented here, we are certain that the model was trained on well distributed data regarding steel strip and anode material. The steel strip and anode material might get changed in the future and model re-training could be necessary to improve generalization of the presented model.

Conclusion

In this paper, we presented a hybrid machine learning approach to predict baseline voltage in a rectifier placed in an electro galvanizing production line and compared it to a simplified physical voltage model. The difference of the baseline from the measured voltage presents parasitic resistance due to bad anode condition. Therefore, this parasitic resistance is employed as an indicator of the anode condition. The best model (a hybrid machine learning model) shows good predictive quality with an RMSE of 0.263 V in a rectifier with (mean \pm std. dev.) 11.228 ± 2.525 V. The winning algorithm RF can easily be employed semi-online (needs periodical re-training) due to fast and parallelizable training and little

preprocessing effort. The final goal is to support the business unit and optimize anode maintenance in a data-driven manner. An early change of aged anodes will save electrical energy as well reduce downtimes and personnel effort, which are all costly. The model can be used for online monitoring of the anode condition, which results in a predictive maintenance approach for anode change. The proposed concept can be transferred to any condition monitor and production setting with or without prior knowledge from machine learning models.

Supplementary information

Supplementary information accompanies this paper at <https://doi.org/10.1186/s40323-020-00184-z>.

Additional file 1. Additional figure, table, data and a detailed physical model.

Acknowledgements

Not applicable.

Authors' contributions

ML—Data curation, Investigation, Writing, Machine learning; RM—Methodology, Investigation, Writing, Physical model; TS—Methodology, Investigation, Writing, Physical model; LF—Data curation, Visualization, Machine learning; JG—Methodology, Validation, Writing, Physical model; SS—Methodology, Validation, Writing; LS—Data curation, Methodology, Validation, Physical model development; SL—Project administration, Supervision, Review and editing; RK—Methodology, Project administration, Supervision, Writing, Review and editing. All authors read and approved the final manuscript.

Funding

The Know-Center is funded within the Austrian COMET Program – Competence Centers for Excellent Technologies – under the auspices of the Austrian Federal Ministry of Transport, Innovation and Technology, the Austrian Federal Ministry of Economy, Family and Youth and by the State of Styria. COMET is managed by the Austrian Research Promotion Agency FFG.

Availability of data and materials

Due to confidentiality reasons, the data cannot be published.

Competing interests

The authors declare that they have no conflict of interest.

Author details

¹ Institute of Interactive Systems and Data Science, TU Graz, Inffeldgasse 16c, 8010 Graz, Austria. ² Know-Center, Inffeldgasse 13/6, 8010 Graz, Austria. ³ Voestalpine Stahl GmbH, 4020 Linz, Austria.

Received: 8 August 2020 Accepted: 29 October 2020

Published online: 18 November 2020

References

- Karner W, Maresch G. Gravitel process for electrogalvanising steel strip. *Steel Time Int.* 1992;17:44–5.
- Karner W, Lavric T, Gerdenitsch J, Faderl J, Wiesinger S. Electro Galvanizing - There Is Life in the Old Dog Yet. *Galvat-ech* 11. Genua; 2011.
- Zhou P, Song H, Wang H, Chai T. Data-driven nonlinear subspace modeling for prediction and control of molten iron quality indices in blast furnace ironmaking. *IEEE Trans Control Syst Technol.* 2017;25:1761–74.
- Liu X, Liu Y, Zhang M, Chen X, Li J. Improving stockline detection of radar sensor array systems in blast furnaces using a novel encoder–decoder architecture. *Sensors (Switzerland).* 2019;19:1.
- Faizullin A, Zymbler M, Liefucht D, Fanghanel F. Use of Deep Learning for Sticker Detection during Continuous Casting. *Proc - 2018 Glob Smart Ind Conf GloSIC 2018.* Institute of Electrical and Electronics Engineers Inc.; 2018.
- Pan ZS, Zhou XH, Chen P. Development and application of a neural network based coating weight control system for a hot-dip galvanizing line. *Front Inf Technol Electron Eng.* 2018;19:834–46.
- Gonzalez-Marcos A, Alba-Elias F, Castejon-Limas M, Ordieres-Mere J. Development of neural network-based models to predict mechanical properties of hot dip galvanised steel coils. *Int J Data Mining, Model Manag.* 2011;3:389–405.
- Groensfelder T, Giebeler F, Geupel M, Schneider D, Jaeger R. Application of machine learning procedures for mechanical system modelling: capabilities and caveats to prediction-accuracy. *Adv Model Simul Eng Sci.* 2020. <https://doi.org/10.1186/s40323-020-00163-4>.
- Fernández M, Rezaei S, Rezaei Mianroodi J, Fritzen F, Reese S. Application of artificial neural networks for the prediction of interface mechanics: a study on grain boundary constitutive behavior. *Adv Model Simul Eng Sci.* 2020;7:1–27. <https://doi.org/10.1186/s40323-019-0138-7>.
- Chen J, Randall R, Peeters B, Desmet W, Van Der Auweraer H. Artificial neural network based fault diagnosis of IC engines. *Key Eng Mater.* 2012. p. 47–56.
- Murphey YL, Masrur MA, Chen ZH, Zhang B. Model-based fault diagnosis in electric drives using machine learning. *IEEE/ASME Trans Mechatronics.* 2006;11:290–303.

12. Galvanuskas V, Simutis R, Lübbert A. Hybrid process models for process optimisation, monitoring and control. *Bioprocess Biosyst Eng.* 2004;26:393–400.
13. Aguiar HC, Filho RM. Neural network and hybrid model: A discussion about different modeling techniques to predict pulping degree with industrial data. *Chem Eng Sci.* 2001;56:565–70.
14. Wu JL, Xiao H, Paterson E. Physics-informed machine learning approach for augmenting turbulence models: A comprehensive framework. *Phys Rev Fluids.* American Physical Society; 2018. p. 7.
15. Wu S, Kondo Y, Kakimoto M, Yang B, Yamada H, Kuwajima I, et al. Machine-learning-assisted discovery of polymers with high thermal conductivity using a molecular design algorithm. *NPJ Comput Mater.* 2019;5:1.
16. Li Y, Yang K. High-throughput computational design of organic-inorganic hybrid halide semiconductors beyond perovskites for optoelectronics. *Energy Environ Sci.* 2019;12:2233–43.
17. Sadoughi M, Hu C. A physics-based deep learning approach for fault diagnosis of rotating machinery. In: *Proc IECON 2018 - 44th Annu Conf IEEE Ind Electron Soc.* Institute of Electrical and Electronics Engineers Inc.; 2018. p. 5919–23.
18. Majda AJ, Harlim J. Physics constrained nonlinear regression models for time series. *Nonlinearity.* 2013;26:201–17.
19. Cao BT, Freitag S, Meschke G. A hybrid RNN-GPOD surrogate model for real-time settlement predictions in mechanised tunnelling. *Adv Model Simul Eng Sci.* 2016;3:5.
20. Stewart R, Ermon S. Label-Free Supervision of Neural Networks with Physics and Domain Knowledge. 2016. <https://arxiv.org/abs/1609.05566>. Accessed 27 Jan 2020.
21. Karpatne A, Atluri G, Faghmous JH, Steinbach M, Banerjee A, Ganguly A, et al. Theory-guided data science: A new paradigm for scientific discovery from data. *IEEE Trans Knowl Data Eng.* 2017;29:2318–31.
22. Karpatne A, Watkins W, Read J, Kumar V. How Can Physics Inform Deep Learning Methods in Scientific Problems?: Recent Progress and Future Prospects. *Talk.* 2017;1–22. https://dl4physicsciences.github.io/files/nips_dmps_2017_19.pdf
23. Lei D, Chen X, Zhao J. Opening the black box of deep learning. 2018. <https://arxiv.org/abs/1805.08355>. Accessed 27 Jan 2020.
24. Lovrić M, Fadljević L, Kern R, Steck T, Gerdenitsch J, Peche E. Prediction of anode lifetime in electro galvanizing lines by big data analysis. *GALVATECH 2020.* Vienna; 2020/ https://www.researchgate.net/publication/340816111_PREDICTION_OF_ANODE_LIFE_TIME_IN_ELECTRO_GALVANIZING_LINES_BY_BIG_DATA_ANALYSIS. Accessed 21 Apr 2020.
25. Maresch G, Ulrich K. US5637205A - Process for the electrolytical coating of an object of steel on one or both sides - Google Patents. 1992.
26. Eisenkoeck P, Lavric T. The GRAVITEL process for electro-galvanising of steel strip. *Millenium Steel.* 2009;141–4.
27. Šimić I, Lovrić M, Godec R, Kröll M, Bešlić I. Applying machine learning methods to better understand, model and estimate mass concentrations of traffic-related pollutants at a typical street canyon. *Environ Pollut.* 2020;263:114587.
28. Haynes WM, editor. *CRC handbook of chemistry and physics*, 93rd edition. CRC Press. 2012
29. Walsh FC. Kinetics of electrode reactions: part I - general considerations and electron transfer control. *Trans Inst Met Finish.* 1992;70:50–4.
30. Bán A, Buttler A, Gerdenitsch J, Debeaux M, Koll T, Lavric T, et al. Energie- und ressourceneffiziente galvanische Bandverzinkung. *ZVO Oberflächentage 2017 [Internet].* Berlin, Germany; 2017. Available from: <http://www.bfi.de/en/lectures/energie-und-ressourceneffiziente-galvanische-bandverzinkung/>
31. Žuvela P, Lovric M, Yousefian-Jazi A, Liu JJ. Ensemble Learning Approaches to Data Imbalance and Competing Objectives in Design of an Industrial Machine Vision System. *Ind Eng Chem Res.* 2020;59:4636–45. <https://doi.org/10.1021/acs.iecr.9b05766>.
32. Bustillo A, Diez-Pastor JF, Quintana G, García-Osorio C. Avoiding neural network fine tuning by using ensemble learning: Application to ball-end milling operations. *Int J Adv Manuf Technol.* 2011;57:521–32.
33. De Abrial IM, Sugiyama M. Winning the Kaggle Algorithmic Trading Challenge with the composition of many models and feature engineering. *IEICE Trans Inf Syst.* Institute of Electronics, Information and Communication, Engineers, IEICE; 2013;E96-D:742–5.
34. Niculescu-Mizil A, Perlich C, Swirszcz G, Sindhwani V, Liu Y, Melville P, et al. Winning the KDD cup orange challenge with ensemble selection. 2009 *Knowl Discov Data Compet (KDD Cup 2009) Challenges Mach Learn.* 2009;7:21. <https://eprints.pascal-network.org/archive/00009182/01/CiML-v3-book.pdf#page=33%5Cnpapers2://publication/uuid/CB992E55-3BD1-40A7-B8E9-FF8922400991>
35. Wold S, Sjöström M, Eriksson L. PLS-regression: A basic tool of chemometrics. *Chemom Intell Lab Syst.* Elsevier; 2001. p. 109–30.
36. Said M, Abdellafou K, Taouali O. Machine learning technique for data-driven fault detection of nonlinear processes. *J Intell Manuf.* 2019. <https://doi.org/10.1007/s10845-019-01483-y>.
37. Breiman L. Random forests. *Mach Learn.* 2001;45:5–32.
38. Freund Y, Schapire RE. Experiments with a New Boosting Algorithm. *Mach Learn Proc Thirteen Int Conf.* 1996. p. 148–56.
39. Pedregosa F, Michel V, Grisel O, Blondel M, Prettenhofer P, Weiss R, et al. Scikit-learn: Machine Learning in Python. *J Mach Learn Res.* 2011;12:2825–30. <https://scikit-learn.sourceforge.net>.
40. Lovrić M, Molero JM, Kern R. PySpark and RDKit: Moving towards Big Data in Cheminformatics. *Mol Inform.* Wiley-VCH Verlag; 2019. p. 38.
41. Lerman PM. Fitting segmented regression models by grid search. *Appl Stat.* 1980;29:77. <https://doi.org/10.2307/2346413?origin=crossref>.
42. Lovrić M, Pavlović K, Žuvela P, Spataru A, Lučić B, Kern R, et al. Machine learning in prediction of intrinsic aqueous solubility of drug-like compounds: generalization, complexity or predictive ability? *ChemRxiv*; 2020.

Publisher's Note

Springer Nature remains neutral with regard to jurisdictional claims in published maps and institutional affiliations.